ELSEVIER

Surface Science 441 (1999) 373–383

surface science

www.elsevier.nl/locate/susc

Comparative theoretical study of the Ag–MgO (100) and (110) interfaces

Yu.F. Zhukovskii [a,b], E.A. Kotomin [a,c,*], P.W.M. Jacobs [b], A.M. Stoneham [d], J.H. Harding [d]

[a] *Institute of Solid State Physics, University of Latvia, Kengaraga 8, LV-1063 Riga, Latvia*
[b] *Department of Chemistry, University of Western Ontario, London, Ont. N6A 5B7, Canada*
[c] *Fachbereich Physik, Universität Osnabrück, Barbarastrasse 7, D-49069, Osnabrück, Germany*
[d] *Centre for Materials Research, Department of Physics and Astronomy, University College London, Gower Street, London WC1E 6BT, UK*

Received 9 April 1999; accepted for publication 16 July 1999

Abstract

We have calculated the atomic and electronic structures of Ag–MgO(100) and (110) interfaces using a periodic (slab) model and an ab initio Hartree–Fock approach with a posteriori electron correlation corrections. The electronic structure information includes interatomic bond populations, effective charges, and multipole moments of ions. This information is analyzed in conjunction with the interface binding energy and the equilibrium distances for both interfaces for various coverages. There are significant differences between partly covered surfaces and surfaces with several layers of metal, and these can be understood in terms of electrostatics and the electron density changes.

For complete monolayer (1:1) coverage of the perfect MgO(100) surface, the most favorable adsorption site energetically for the Ag atom is above the surface oxygen. However, for partial (1:4) coverage of the same surface, the binding energies are very close for all the three likely adsorption positions (Ag over O, Ag over Mg, Ag over a gap position).

For a complete (1:1) Ag monolayer coverage of the perfect MgO(110) interface, the preferable Ag adsorption site is over the interatomic gap position, whereas for an Ag bilayer coverage the preferred Ag site is above the subsurface Mg^{2+} ion (the bridge site between two nearest surface O^{2-} ions). In the case of 1:2 layer coverage, both sites are energetically equivalent. These two adhesion energies for the (110) substrate are by a factor of two to three larger than over other possible adsorption sites on perfect (110) or (100) surfaces.

We compare our atomistic calculations for one to three Ag planes with those obtained by the shell model for 10 Ag planes and the Image Interaction Model addressing the case of thick metal layers. Qualitatively, our ab initio results agree well with many features of these models. The main charge redistributions are well in line with those expected from the Image Model. There is also broad agreement in regard to orders of magnitude of energies. © 1999 Elsevier Science B.V. All rights reserved.

Keywords: (100) and (110) interfaces; Adhesion; Adsorption; Ag–MgO; Hartree–Fock method; Image interaction model

* Corresponding author. Fax: +371-711-2583.
E-mail address: kotomin@latnet.lv (E.A. Kotomin)

0039-6028/99/$ – see front matter © 1999 Elsevier Science B.V. All rights reserved.
PII: S0039-6028(99)00847-X

1. Introduction

The understanding and control of metal–ceramic interfaces underpins many technological applications (see Refs. [1–25] and references cited therein). These interfaces are often very complex. One example might be the interface between a nuclear fuel (basically UO_{2+x} with fission products) in contact with the alloy clad. There is, therefore, a substantial gap between the basic science of idealized interfaces and the formulations that can be used by engineers. In the case of metal–ceramic interfaces, the phenomenological Image Interaction Model (IIM) [11] could bridge this gap, and one of our aims is to check and validate some of the ideas within that description. We shall also link our results to experiment, notably to high-resolution electron microscopy measurements, which give data for a few metal–oxide (e.g. Ag–MgO) interfaces [26,27] at near-atomic resolution.

For liquid-metal–oxide interfaces, a small adhesion energy is associated with a large wetting angle. Wetting (small wetting angle) is often found when there is a chemical reaction between the liquid metal and the oxide substrate. For non-reactive liquid metals, there are systematic trends of wetting angle with substrate [11]. For Ag–MgO, our calculation shows negligible chemical reaction with perfect MgO surfaces. The major terms in adhesion must, therefore, correspond to a physical mechanism, for instance the polarization of the metal by the oxide ions, which underlies the Image model. What is seen for solid metal films on oxides depends strongly on growth conditions, at least for thin metal layers on an oxide substrate. Thus, Ag growth on MgO usually gives rise to three-dimensional islands [26–28]. On the other hand, a recent low-energy electron diffraction study indicates a layer-by-layer growth mode for silver deposits on vacuum-cleaved MgO(100) surfaces, even though such a structure is metastable [29,30]. Part of the explanation will lie in kinetics, the rate of Ag deposition and the competition between different surface processes [31]. It is also clear that defects can play a crucial role in determining the epitaxial growth mode [32–34]. This is supported by calculations [35] that show a delicate energy balance between Ag island and monolayer-mode growth.

Despite the existence of many theoretical studies of the adhesion of noble and transition metals on MgO substrates [11,32–46], a full understanding of interface formation and of properties on an atomic scale is still lacking. Partly this is because of some very sensitive balances between contributions to the energy. Indeed, it is arguable that the successes are more surprising than the inconsistencies. This is especially true when the range of methods is recognized. *Cluster* models [32–34,42,43] and *slab* models (periodic in two dimensions) [36–41] have been used; a few calculations have attempted proper *embedding* [23]. An ab initio Hartree–Fock formalism has been used in cluster calculations of some Me–MgO interfaces [32–34]. The local density approximation (LDA), as implemented in a full-potential linearized muffin-tin orbital method (FP LMTO), has been applied in a slab model for metal adhesion on the MgO surfaces [36–38], as have full-potential linearized augmented plane waves (FP LAPW) [39], and self-consistent local orbitals (LO) [40–43]. In order to go beyond the LDA approximation for metal–oxide interfaces, we recently made preliminary Hartree–Fock calculations for the Ag–MgO (100) interface using a slab model [44,45].

In addition to the methods that calculate electronic structure explicitly, two other atomistic methods have been used with success for these interfaces: the atomistic shell model (SM) [46] and the IIM [11,12]. The latter model has sufficient simplicity for application to those very complex systems that are important technologically.

In this paper, we give the first comparative ab initio study of the Ag–MgO(100) and (110) interfaces based on a quantitative analysis of the bonding in the interfacial region. We shall describe the way in which interfacial electronic and other properties evolve as a function of metal coverage.

2. Theoretical

2.1. Computational details

We use the ab initio Hartree–Fock computer code CRYSTAL-95 for periodic systems [47],

which incorporates electron correlation corrections (hereafter termed the HF-CC method). These corrections were calculated using density-functional theory [48]. Such terms are necessary, since standard Hartree–Fock theory underestimates binding energies and overestimates bond lengths of molecules. In the framework of the HF-CC method, we used Perdew–Wang a posteriori corrections [49]. The basis set for MgO, optimized elsewhere [50], consists of all-electron 8-61G and 8-51G functions (s and sp shells) for Mg and O atoms respectively. To reduce computational efforts, we employed the small-core Hay–Wadt pseudopotentials for Ag atoms [51], thus reducing the total number of electrons per Ag atom to 19 ($4s^2 4p^6 4d^{10} 5s^1$). An initial guess for the basis set of bulk silver (311-31G for sp and d shells) was taken from AgCl calculations [52], and the outer exponents were re-optimized [44,45]. Calculations starting with the Ag $4d^9 5s^2$ configuration give essentially the same results.

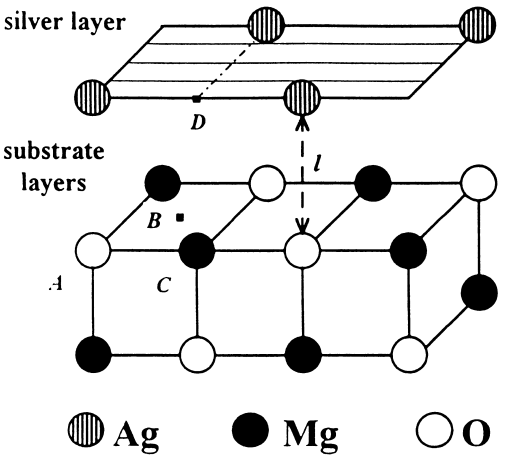

Fig. 1. Fragment of the Ag–MgO (100) interface where Ag atoms are placed at the distance *l* above O atoms of the substrate surface (*A* configuration). Two other possible adsorption positions are above the gap (*B*) and Mg atoms (*C*). Additional atomic wave functions in the Ag slab are centered in its hollow sites (*D*).

2.2. The model of the Ag–MgO (100) interface

The CRYSTAL-95 computer code allows calculations on finite-thickness slabs as two-dimensional periodic systems. We have simulated the Ag–MgO(100) interface (Fig. 1) with either one Ag monolayer or three Ag layers atop three layers of the oxide substrate. For the monolayer, we have considered full coverage [a complete (1:1) substrate] and partial (1:4) Ag coverage.

The optimized value of the lattice constant for the three-layer MgO slab (4.21 Å [44]) is very close to the experimental bulk value (4.205 Å [50]). In line with all previous calculations, we ignore the small (3%) mismatch in the lattice constants of fcc Ag (4.08 Å [53]) and MgO, although we recognize that this leads to mismatch dislocations when we compare with experiment. In our calculations, we fix the lattice constant along the surface *xy* plane at 4.21 Å, and allow only the interfacial (metal–substrate) distance to vary along the *z* axis, perpendicular to the interface. The distances between different silver planes within the metal slab are also free to change (for the three-layer Ag(100) slab they were optimized to be 1.98 Å [45]). We have obtained results in this way for all three of the most likely sites for Ag adsorption: above surface Mg^{2+} ions (*C*), above surface O^{2-} ions (*A*), and in the interatomic gaps (*B*) shown in Fig. 1. In calculations for the (1:1) Ag coverage of the perfect MgO(100) surface we have also used additional atomic wave functions (to give greater variational freedom [44,45]) centered in hollow sites *D* in the Ag slabs (Fig. 1). A preliminary optimization of their basis set 1(sp)–1(d)G was carried out for bulk silver [45].

2.3. The Ag–MgO(110) interface model

For complete (1:1) coverage of the perfect MgO(110) surface, we have simulated the adhesion both of an Ag monolayer and an Ag bilayer on a three-layer MgO substrate (Fig. 2). A previous study of MgO(110) [54] revealed that three planes sufficed for geometry and surface energy optimization. The adhesion energy (we defined it elsewhere [44,45]) has been optimized for all five potential sites for Ag atom adsorption: above surface Mg^{2+} or O^{2-} ions, above subsurface Mg^{2+} or O^{2-} ions, and in the interatomic gap. As for the Ag–MgO(100) interface, we have both ignored the small lattice mismatch between fcc Ag and MgO and optimized the interlayer distance in

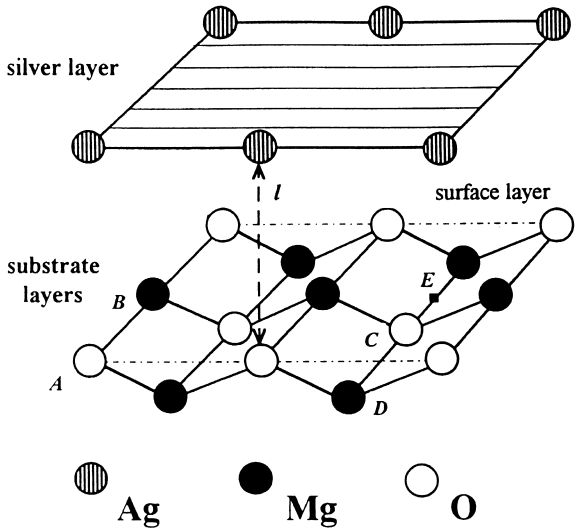

Fig. 2. Fragment of the Ag–MgO (110) interface where Ag atoms are positioned above O atoms of the substrate surface (*A* configuration). Four other possible positions are above surface Mg atoms (*B*), subsurface O and Mg atoms (*C* and *D* respectively) as well as the gap (*E*). In the figure, the interlayer spacing in the MgO(110) slab is somewhat compressed, whereas the interface spacing *l* is slightly expanded to aid visualization.

the bilayer Ag(110) slab. To simulate a partial (1:2) substrate coverage by silver atoms, we have used a 1×2 extended Ag layer along the [110] axis (this is parallel to the strips on the Ag layer shown in Fig. 2), so that there are alternating equivalent sites that are occupied or unoccupied by Ag atoms. Unlike the perfect MgO(100) substrate, where every surface ion is surrounded by five dissimilar ions, the atoms on the (110) surface are fourfold coordinated: surface rows along the [110] direction contain only cations or only anions. Taking into account the fact that the surface energy of less densely packed MgO(110) is larger than for MgO(100) [54], one expects stronger adsorbate binding. This was indeed found for CO molecular adsorption [54].

3. Results and discussion

3.1. Adhesion on the MgO (100) surface

Table 1 and Fig. 3. summarizes our main results. First, we consider the favored adsorption site for Ag. For full (1:1) coverage, whether there are one or three layers of Ag, adsorption over the surface O atoms is most favorable energetically. This agrees with recent experiments [55] and with three previous LDA-type calculations [36–39]. It contradicts those IIM results [20,23] for which the most accurate treatment of the dispersion forces is included, but agrees with the Image Model (IM) approach with a less-accurate treatment of dispersion. The main difference for the IIM appears to be associated with the strength of the long-range dispersion forces between the Ag and the O neighbors of the Mg site below the Ag.

For the favored *A* configuration (Ag over O; see Fig. 1) the equilibrium interface distances calculated for all the microscopic methods are reasonably close, falling into narrow range between 2.5 and 2.7 Å; the IM also agrees, giving 2.53 Å. Our HF-CC value of 2.43 Å for three metal layers coincides with the recent experimental data [55].

We have examined the effects of extending the basis set to include special atomic wave functions (Section 2.2) in the hollow positions *D* of the Ag slab (Fig. 1). Their effect is to strengthen slightly the interfacial binding and to bring the metallic film and oxide substrate closer. The effect is largest for the *A* configuration, where the change is 0.08 Å (about 3%). As a result, the adhesion energy per Ag atom in the monolayer is increased. Our monolayer adhesion energy of 0.25 eV is close to the value of 0.30 eV obtained for the same structure in the FP LAPW calculations [39] (Table 1). On the other hand, an increase in the number of Ag planes to three increases the HF-CC adhesion energy over O atoms to 0.46 eV, but does not affect much the adhesion for Ag over a gap or over an Mg atom. Nevertheless, our value of 0.46 eV is smaller than the adhesion energy of 0.88 eV found in FP LMTO calculations on the same interfacial structure (three Ag layers) [36]. The relevant experimental estimate is 0.26 eV [26,27], which is probably lower due to the presence of misfit dislocations caused by the 3% difference in lattice parameters of Ag and MgO (Fig. 3).

Chemical bonding across the interface between metal and oxide substrate is negligible: the adhesion is physical in origin. The calculated Mulliken charges on Ag atoms indicate negligible charge

Table 1
Optimized parameters for the Ag–MgO(100) interface. The relevant adsorption positions are shown in Fig. 1

Ag atom over	Coverage	Additional functions[a]	Distance $l^{(o)}$ (Å)	Adhesion E_{adh} (eV)	Charge[b] $e(00)_{Ag}$ (e)	Dipole[c] $d(10)_{Ag}$ ($e\,a_o$)	Quadrupole[c] $q(20)_{Ag}$ ($e\,a_o^2$)
O atom (A)	$\frac{1}{4}$ layer	none	2.58	0.23	0.063	0.251	−0.433
	Single Ag layer	none	2.64	0.20	0.028	0.130	−2.052
		included	2.56	0.26	0.037	0.198	−2.232
	3 layers	included	2.43	0.46	0.053[d]	0.418[d]	−1.971[d]
	SM[e]		2.60	0.11	–	–	–
	IIM[f]		2.53	0.30			
Interatomic gap (B)	$\frac{1}{4}$ layer	none	2.69	0.20	0.052	−0.007	0.140
	Single Ag layer	none	3.00	0.10	0.025	−0.038	−1.408
		included	2.94	0.15	0.035	−0.034	−1.597
	3 layers	included	2.86	0.17	0.050[d]	0.182[d]	−0.963[d]
	IIM[f]		2.53	0.48			
Mg atom (C)	$\frac{1}{4}$ layer	none	2.89	0.22	0.038	−0.170	0.414
	Single Ag layer	none	3.24	0.06	0.015	−0.065	−1.314
		included	3.23	0.06	0.027	−0.071	−1.288
	3 layers	included	3.23	0.07	0.042[d]	0.116[d]	−0.686[d]
	SM[e]		3.20	0.02	–	–	–
	IIM[f]		2.74	0.60			

[a] Additional atomic wave functions centered in hollow sites D (Fig. 1).
[b] Positive sign means excess of the electron density compared with a neutral atom.
[c] The values of dipole and quadrupole moments are given in atomic units (1 a_o = 1 Bohr).
[d] For the interfacial silver layer.
[e] The shell model calculations [46] for 10 Ag layers atop 31 MgO planes.
[f] The IIM [20,23].

transfer between MgO and Ag [see the $e(00)$ column in Table 1]. The bond populations across the interface [between Ag atoms and ions of the perfect MgO(100) substrate] are practically zero. We remark that the existence of a good fit [40,41] of the interfacial energy versus interface distance to the so-called *universal binding energy relation* (similar to the potential energy curve for diatomic molecule) does not necessarily imply chemisorption between metal and substrate (see more in Ref. [45]).

On the other hand, there is redistribution of charge *within* the metal. We observe considerable bond populations between nearest Ag atoms (0.1e per atom) within the metal planes parallel to the interface. This population is not sensitive to the adsorption site. The concentration of the electron density in the Ag at the *bridge position* between nearest metal atoms has been confirmed recently in inelastic He scattering studies [56]; only by introducing negative pseudo-charges in these positions in metal films could a good fit be found for theoretical surface phonon-dispersion curves to experimental data.

The bond population analysis, already mentioned, gives a reason for Ag adsorption over O^{2-} ions to be favored. This preference is related to electrostatic attraction involving the enhanced Ag electron density concentrated around the hollow position in the interfacial Ag layer (0.07e for the 1:1 Ag coverage). The extra charge has an attractive interaction with the substrate Mg^{2+} ion below it (Fig. 1). On the other hand, for the Ag adsorption over the Mg^{2+} ions, there is instead repulsion between the electron density localized in the D position and the substrate O^{2-} ion below it.

The atomic dipole moments $d(10)$ in Table 1 are calculated as matrix elements of the atomic orbitals with the operator z (the direction pointing outwards from the surface) [47,54]. They characterize a shift of electron density along the z axis. As expected from the IIM, the dipoles have oppo-

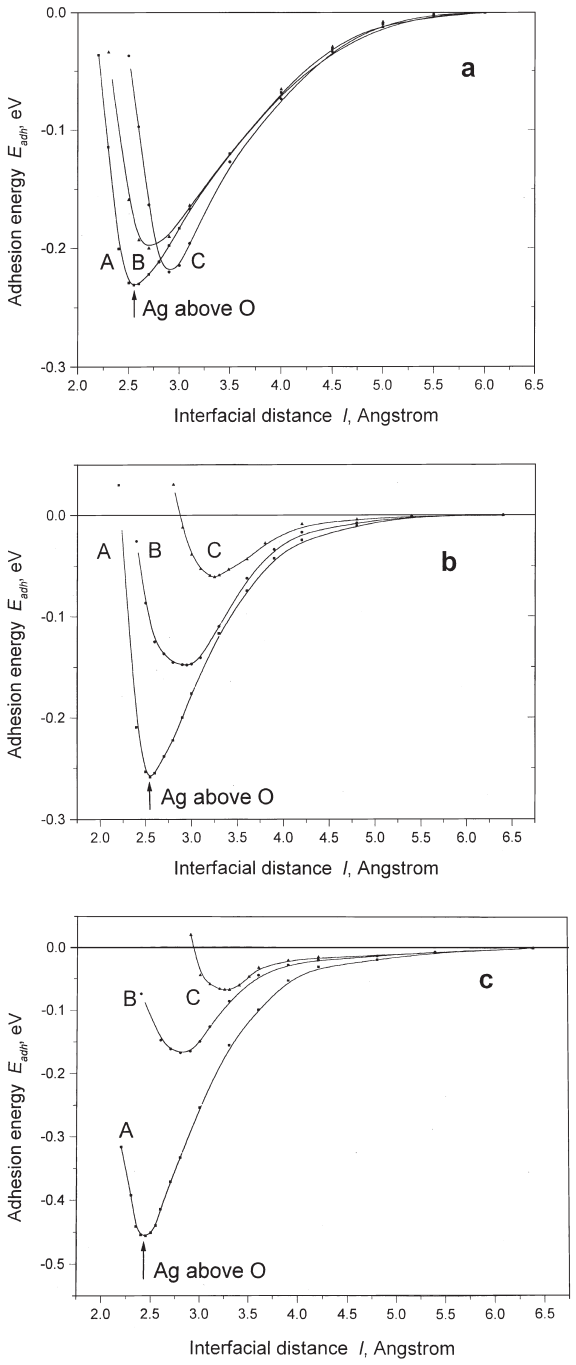

Fig. 3. The interfacial energies for different adsorption sites for Ag atoms on the perfect MgO(100) surface as a function of the distance l between adsorbent and adsorbate (Fig. 1). Three different substrate coverages by silver: $\frac{1}{4}$ layer (a), monolayer (b) and three layers (c) (with additional atomic wave functions included for the two latter cases) are studied. Full lines are drawn using the standard b-spline option. See notations of the adsorption positions in Fig. 1.

site signs above O and above Mg, corresponding to electrons being repelled by the anion or attracted by the cation. For the Ag monolayer, the dipole moment is largest for Ag over the (optimal) O site. The quadrupole moments $q(20)$ in Table 1 are matrix elements with the operator $z^2-(x^2+y^2)/2$, and also characterize atomic deformation. These moments are affected significantly by Ag 4d–5s orbital mixing. A negative $q(20)_{Ag}$ (as found in almost all cases except the $\frac{1}{4}$ layer) means the Ag has contracted axially (z direction) and expanded in the xy plane. For all adsorption positions, magnitudes for Ag atoms are at least a factor four larger than the corresponding magnitudes for surface Mg^{2+} and O^{2-} ions. Thus, Ag atoms adsorbed on the MgO(100) surface are considerably deformed.

The larger adhesion energy for three Ag layers, compared with an Ag monolayer, can be attributed to a more complicated electron density distribution in the interfacial Ag layer for both the A and C interfacial configurations. For the A adsorption site, a charge of $0.04e$ is localized on the corresponding hollow position over Mg^{2+}, whereas $0.12e$ is localized on each of the four side bridge positions in the plane above the D point. For the C adsorption site, the corresponding electron densities over O^{2-} are smaller ($0.03e$ and $0.1e$ respectively) and much more remote from the surface oxygen ion. There may be a similar explanation for the additional increase of the adhesion energy when introducing atomic orbitals at the D positions for both one- and three-layer Ag slabs. The effective atomic charges and their definitions are discussed further in Ref. [56].

For partial (1:4) Ag coverage of the MgO(100) surface there are differences from both the monolayer and three layer (1:1) coverages. For such a low coverage there is practically no interatomic electron density concentration between Ag atoms; therefore, its interaction or repulsion with the nearest substrate atom plays no role here. For Ag adsorption over O or Mg ions, there is a single nearest substrate ion (either O^{2-} or Mg^{2+}) and four next-nearest substrate ions of the opposite type (either Mg^{2+} or O^{2-}). However, for the gap adsorption site, every Ag atom has four nearest

substrate ions (two Mg^{2+} and two O^{2-}). Since adsorption energies of these relatively isolated Ag atoms are close for all three adsorption sites (*A*, *B* and *C*), the difference from full coverage may be explained by a partial compensation of electrostatic attraction and repulsion between slightly charged Ag adatoms and the substrate ions.

For the 1:4 surface coverage, charge transfer from the substrate to each isolated Ag atom is small (0.06*e*), yet it is still twice as large as for the Ag monolayer or for three Ag layers atop MgO. The value of the dipole moment for the Ag atom is also twice as large for 1:4 as it is for 1:1 coverage. The isolated Ag atom charge density is deformed along the *z* axis as expected in the IM model. On the other hand, the quadrupole moment is significantly smaller for a single Ag than that for a monolayer, which shows that its non-spherical deformation due to the field gradient of the MgO ions is small (Table 1). This difference may be associated with the mismatch of Ag and MgO lattice spacings, which is a bigger effect for full coverage situations. Fig. 4 shows the difference electron density maps for low Ag coverage over O and Mg ions. This demonstrates that Ag atoms are more polarized above O substrate ions where the charge transfer from the substrate is greater. Various difference electron density maps were discussed by us earlier for the cases of one [44] and three [45] Ag layers above the MgO(100) substrate.

We have calculated the effects of the basis-set-superposition-error (BSSE) [57]. If no atomic wave functions are centered on the hollow position, the effect is negligible (0.005 eV). Even when they are included, the BSSE remains small: it is only 0.03 eV for Ag above O.

Recent SM calculations [46] also predict preferential adsorption over O ions, but with an adhesion energy of only 0.11 eV — smaller than our predictions. This smaller value may result from the neglect of the electron density redistribution within the metal plane. We suspect that an important part of the differences in detail between full electronic structure calculations and these simpler approaches stems from the relatively subtle shifts in charge density in the Ag.

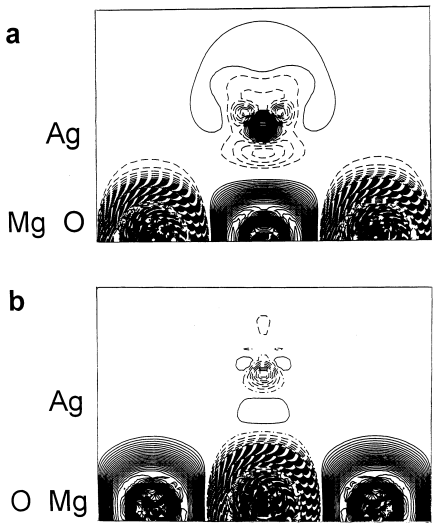

Fig. 4. The *difference* electronic density maps (the total density minus superposition of atomic densities) or the cross-section perpendicular to the (100) interface plane for $\frac{1}{4}$ Ag adsorption: (a) over O and (b) over Mg ions. Isodensity curves are drawn from -1 to $+1e\,a_o^{-3}$ with an increment of $0.0015e\,a_o^{-3}$. The full, dashed and chained curves show positive, negative and zero difference densities respectively. Note that Ag atoms are strongly polarized: above O ions (a) the electron density is shifted in the direction outwards from the surface, whereas above Mg (b) it is shifted towards surface Mg ions.

3.2. Adhesion on perfect MgO (110) surface

The basic properties for the Ag–MgO(110) interface are summarized in Table 2 and Fig. 5. Unlike the Ag–MgO(100) interface, the preference for one adsorption site rather than another depends on the Ag coverage. One can conclude only that certain sites for Ag ('bridge O', 'above gap' and 'atop O', the *D*, *E* and *A* sites on Fig. 2 respectively) are much more favorable than certain other sites ('bridge Mg' and 'atop Mg' sites, *C* and *B* respectively). This conclusion confirms results obtained earlier by the SM for the same Ag–MgO(110) interface [46], which gave the 'atop O' site priority over the 'atop Mg' site, and are in agreement with our previous HF-CC calculations for the Ag–MgO(100) interface [44,45]. The equilibrium interface distances are much smaller for the preferred Ag adsorption sites than for other sites on MgO(110) (Table 2). The quadrupole atomic moments for these sites, $q(20)$, are evi-

Table 2
Optimized parameters for the Ag–MgO(110) interface. Adsorption positions (*A* to *E*) are shown in Fig. 2

Interfacial Ag atom over	Coverage	Distance $l^{(o)}$ (Å)	Adhesion E_{adh} (eV)	Charge[a] $e(00)_{Ag}$ (e)	Dipole[b] $d(10)_{Ag}$ ($e\,a_o$)	Quadrupole[b] $q(20)_{Ag}$ ($e\,a_o^2$)
O atom of surface layer (atop O, site *A*)	½ layer	2.35	0.58	0.072	0.474	−1.238
	Monolayer	2.51	0.31	0.049	0.298	−1.645
	Bilayer	2.23	0.94	−0.007[c]	0.637[c]	−2.161[c]
	SM[d]	1.79	0.54	–	–	–
O atom of subsurface layer (bridge Mg, site *C*)	½ layer	2.46	0.31	0.050	−0.363	0.162
	Monolayer	2.52	0.34	0.053	−0.341	−0.435
	Bilayer	2.53	0.18	0.088[c]	−0.05[c]	−0.45[c]
Center between O and Mg atoms (interatomic gap, *E*)	½ layer	1.87	0.82	0.112	0.048	−0.551
	Monolayer	1.93	0.68	0.087	0.022	−1.210
	Bilayer	1.88	0.82	0.088[c]	0.308[c]	−0.785[c]
Mg atom of surface layer (atop Mg, site *B*)	½ layer	2.97	0.16	0.03	−0.281	0.132
	Monolayer	2.92	0.19	0.035	−0.257	−0.467
	Bilayer	3.04	0.09	0.050[c]	0.086[c]	−0.346[c]
	SM[d]	2.40	0.03	–	–	–
Mg atom of subsurface layer (bridge O, site *D*)	½ layer	1.95	0.82	0.076	0.576	−1.203
	Monolayer	2.05	0.38	0.051	0.470	−1.836
	Bilayer	1.75	1.32	−0.092[c]	0.789[c]	−1.833[c]

[a] Positive sign means excess of the electron density compared with a neutral atom.
[b] The values of dipole and quadrupole moments are given in atomic units (1 a_o = 1 Bohr).
[c] For the interfacial silver layer.
[d] The shell model calculations [46] for 10 Ag layers atop 31 MgO layers.

dently larger as well, confirming qualitatively our results for the Ag–MgO(100) interface (Table 1). All kinds of Ag atoms adsorbed on the MgO(110) surface have larger quadrupole moments than on the (100) interface, due to bigger electric field gradients above the (110) surface. (Analyses of the dipole and quadrupole moments for the pure and CO-covered MgO(110) surface are presented in Ref. [54].)

The effects of substrate coverage are similar to those for the Ag–MgO(100) interface (Section 3.1). For a low (1:2) coverage, the electron density is no longer enhanced so much in interatomic positions of the silver film, so that the mechanism of Ag atomic adsorption can be established more directly. An interaction along the Ag—O bond for *A* sites is larger on MgO(110) than on the MgO(100), because in the latter (100) case it is reduced by the interactions with the four Ag—Mg bonds of the first coordination semisphere (Fig. 1). By *bonds* we mean simply a tendency to form Ag—O bonds; despite the fact that there is no pronounced quantitative bond population between the Ag and O atoms, the atoms are polarized towards each other to some extent, as is seen from the electron density maps.

The difference electron density maps at different adsorption positions shown in Fig. 6 clearly demonstrate that the charge density in Ag atoms is changed much more at the O *bridge* (Mg bridge) positions compared with the single O (Mg) ion position, which is confirmed by inspection of Table 2. As for the (100) surface, Ag atoms are more polarized in a position above O ions rather than Mg ions and the charge transfer from the substrate is also greater in the former case. In

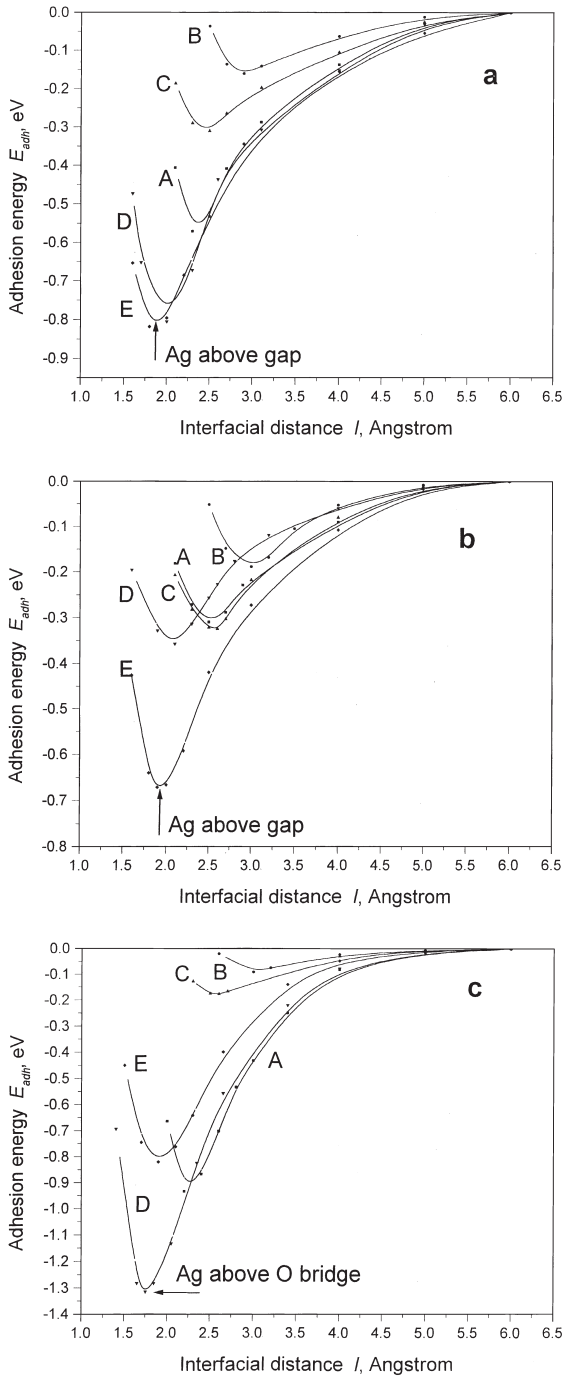

Fig. 5. The interfacial energies for different adsorption sites of Ag atoms on the perfect MgO(110) surface as a function of the distances l between adsorbent and adsorbate (Fig. 2). Three different substrate coverages: half-layer (a), monolayer (b) and bilayer (c) are studied. Full lines are drawn using the standard b-spline option. See notations of the adsorption positions in Fig. 2.

contrast, on Ag–MgO(110) a slight repulsion in two nearest Ag—Mg bonds is partly compensated by the attraction of the two next-nearest Ag—O bonds (Fig. 2). For the bridge O sites (D) and the gap sites (E), the Ag atom interaction with two nearest O^{2-} ions is even more evident.

For *monolayer* Ag coverage of the substrate, there is an electrostatic repulsion between the O^{2-} ions and an interatomic electron density [0.13–0.17e, which may be compared with 0.07–0.1e for the (100) case]. That is why the D and A sites become much less preferred, whereas in the gap site (E) the repulsion of O^{2-} ions and the interatomic density is largely compensated by its attraction to Mg^{2+} ions. Thus, gap sites (E) are the most energetically favored for Ag monolayer substrate coverage.

In the case of an Ag *bilayer* on an MgO(110) surface, the major charge redistribution within the Ag(110) slab occurs over the A and D sites. Electron density is transferred from the interfacial silver layer (next to the MgO) to the outer Ag layer. The bond populations between Ag atoms also change. In the interfacial layer, the bond populations decrease down to 0.02–0.03e, but in the second (outer) layer and between the two Ag planes, the populations increase by up to 0.09–0.1e. As a result, the interfacial Ag atoms have a net *positive* charge, which strengthens their interaction with substrate O^{2-} ions. At the same time, the electrostatic attraction between the interface interatomic electron density and the surface Mg^{2+} ions becomes much smaller for the B and C positions than it was for monolayer coverage. There is no significant change for the gap position E, where there is compensation between attractive and repulsive effects.

Once again, from all results obtained, we can confirm unambiguously that there is no evidence of chemical binding between Ag and MgO(110): adhesion is physisorption. Just as we found for the perfect Ag–MgO(100) interface, the bond populations across the interface [between the Ag atoms and the ions of the perfect MgO(110) substrate] are negligible. This is in line with predictions of the IIM, except perhaps for the inter-Ag charge effects.

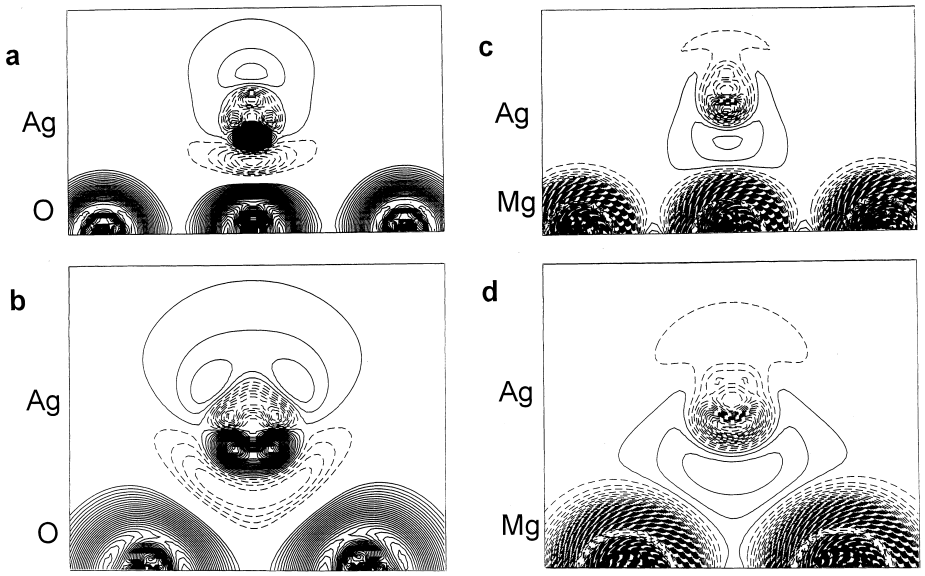

Fig. 6. The *difference* electronic density maps for the cross-section perpendicular to the (110) interface plane for $\frac{1}{4}$ Ag adsorption: (a) over a single O ion, (b) over O bridge, (c) over a single Mg ion, and (d) over Mg bridge position. Isodensity curves are drawn from -1 to $+1e\,a_o^{-3}$ with an increment of $0.0015e\,a_o^{-3}$. The full, dashed and chained curves show positive, negative and zero difference densities respectively. As in Fig. 4, Ag atoms are strongly polarized: above O ions (a,b) the electron density is shifted in the direction outwards from the surface, whereas above Mg (c,d) it is shifted towards surface Mg ions. Note that the electron density for O ions (a,b) is visibly compressed in the Ag directions, compared with the other cases shown.

4. Conclusions

One important general conclusion to be drawn from the ab initio Hartree–Fock calculations is that chemical bond formation is not important for either Ag–MgO(100) or Ag–MgO(110) perfect interfaces. Physical adhesion associated with polarization and charge redistribution are the dominant effects. The adhesion energy is enhanced by the interaction of the substrate ions with the extra electron density near the interatomic positions of the interfacial Ag layer. This favors silver atoms placed above either surface O^{2-} ions for the (100) substrate, or the *bridge* position (the center between nearest oxygen ions) and the *gap* position (the middle between O^{2-} and Mg^{2+} ions) for the (110) surface. The difference in predicted optimal Ag adsorption sites observed for microscopic and the IM stems mainly from the different treatments of long-range dispersion (van der Waals) interactions. However, these two kinds of calculation complement each other, since they address different situations: atomistic modeling focuses on several metal planes, whereas the IM prediction is for a thick metal layer atop an oxide substrate. Is is well known that substrate near-surface defects play a crucial role in metal adsorption on oxide surfaces and in the adhesion energy of metals to oxides as well [23,58–62]. This problem will be addressed in our next paper.

Acknowledgements

This study was supported by both the British-German Academic Collaboration Programme ARC project 88F and a British–Latvian Royal Society Joint Project Grant for collaborations with the former Soviet Union. Y.Z. greatly appreciates the support of the Center for Chemical Physics and of the Department of Chemistry of the University of Western Ontario (Canada) for a Senior Visiting Fellowship and a post-doctoral Fellowship. The authors kindly thank I. Abarenkov, M. Causá, D.M. Duffy, E. Heifets, V. Kempter and A.L. Shluger for many stimulating discussions.

References

[1] V.E. Heinrich, P.A. Cox, The Surface Science of Metal Oxides, Cambridge University Press, Cambridge, 1994.
[2] F. Ernst, Mater. Sci. Eng. R14 (1995) 97.
[3] M.W. Finnis, J. Phys.: Condensed Matter 8 (1996) 5811.
[4] C.T. Campbell, Surf. Sci. Rep. 27 (1997) 1.
[5] G. Renaud, Surf. Sci. Rep. 32 (1998) 1.
[6] H.-J. Freund, M. Bäumer, J. Libuda, H. Kuhlenbeck, T. Risse, K. Al-Shamery, H. Hamann, Crystallogr. Res. Tech. 33 (1998) 977.
[7] A.M. Stoneham, P.W. Tasker, in: J.A. Pask, A.G. Evans (Eds.), Ceramic Microstructures '86, Plenum, 1987, p. 155.
[8] G. Ertl, H.-J. Freund, Phys. Today (1) (1999) 32.
[9] Proceedings of 4th International Symposium on Atomically Controlled Surfaces and Interfaces, Appl. Surf. Sci. 130–132 (1998)
[10] A.M. Stoneham, J. Harding, T. Harker, Mater. Res. Soc. Bull. 21 (1996) 29.
[11] A.M. Stoneham, Appl. Surf. Sci. 14 (1983) 249.
[12] A.M. Stoneham, P.W. Tasker, J. Phys. C 18 (1985) L543 also Harwell, reprint TP1122.
[13] P.W. Tasker, A.M. Stoneham, J. Phys. (Paris) 84 (1987) 149.
[14] A.M. Stoneham, P.W. Tasker, in: J.A. Pask, A.G. Evans (Eds.), Ceramic Microstructures '87: Role of Interfaces, Plenum, Press, 1986, p. 155.
[15] P.W. Tasker, A.M. Stoneham, Mater. Sci. Eng. 4 (1988) 382.
[16] M.W. Finnis, A.M. Stoneham, P.W. Tasker, in: M. Rühle (Ed.), Metal–Ceramic Interfaces, Pergamon, Oxford, 1990, p. 35.
[17] A.M. Stoneham, P.W. Tasker, in: S.D. Peteves (Ed.), Designing Interfaces for Technological Applications vol. 16 , Elsevier, 1989, p. 217.
[18] A.M. Stoneham, D.M. Duffy, J.H. Harding, P.W. Tasker, in: S.D. Peteves (Ed.), Designing Ceramic Interfaces, CEC Directorate General, Science Research and Development, 1993, p. 573. also AEA-InTec-0708.
[19] D.M. Duffy, J.H. Harding, A.M. Stoneham, Acta Metall. Mater. 40 (Suppl.) (1992) S11.
[20] D.M. Duffy, J.H. Harding, A.M. Stoneham appendix by J.R. Willis, Philos. Mag. A: 67 (1993) 865.
[21] D.M. Duffy, J.H. Harding, A.M. Stoneham, J. Appl. Phys. 76 (1995) 2791.
[22] A.M. Stoneham, D.M. Duffy, J.H. Harding, in: N. Eustathopoulos (Ed.), High Temperature Capillarity, Slovak Academy of Sciences, 1994, p. 1.
[23] D.M. Duffy, J.H. Harding, A.M. Stoneham, Acta Metall. Mater. 43 (1995) 1559.
[24] J.H. Harding, A.H. Harker, A.L. Shluger, A.M. Stoneham, Acta Metall. Mater. 46 (1998) 2255.
[25] D.M. Duffy, J.H. Harding, A.M. Stoneham, Acta Metall. Mater. 44 (1996) 3293.
[26] A. Trampert, E. Ernst, C.P. Flynn, H.F. Fischmeister, M. Ruhle, Acta Metall. Mater. 40 (1992) S227.
[27] P. Guenard, G. Renaud, B. Vilette, M.-H. Yang, C.P. Flynn, Scr. Metall. Mater. 31 (1994) 1221.
[28] M.-H. Schaffner, F. Patthey, W.-D. Schneider, Surf. Sci. 417 (1998) 159.
[29] T. Harada, M. Asano, Y. Mizutani, J. Cryst. Growth 116 (1992) 243.
[30] F. Didier, J. Jupille, Surf. Sci. 307–309 (1994) 587.
[31] J.H. Harding, A.M. Stoneham, J.A. Venables, Phys. Rev. B 57 (1998) 6715.
[32] N.C. Bacalis, A.B. Kunz, Phys. Rev. B 32 (1985) 4857.
[33] A.M. Ferrari, G. Pacchioni, J. Phys. Chem. 99 (1995) 17 010.
[34] A.M. Ferrari, G. Pacchioni, J. Phys. Chem. 100 (1996) 9032.
[35] A.M. Stoneham, J.H. Harding, Acta Metall. Mater. 46 (1998) 1155.
[36] U. Schönberger, O.K. Andersen, M. Methfessel, Acta Metall. Mater. 40 (1992) S1.
[37] J. Goniakowski, Phys. Rev. B 57 (1998) 1935.
[38] J. Goniakowski, Phys. Rev. B 58 (1998) 1189.
[39] C. Li, R. Wu, A.J. Freeman, C.L. Fu, Phys. Rev. B 48 (1993) 8317.
[40] T. Hong, J.R. Smith, D.J. Srolovitz, J. Adhesion Sci. Technol. 8 (1994) 837.
[41] T. Hong, J.R. Smith, D.J. Srolovitz, Acta Metall. Mater. 43 (1995) 2721.
[42] G. Pacchioni, N. Rösch, J. Chem. Phys. 104 (1996) 7329.
[43] I.V. Yudanov, S. Vent, K. Neyman, G. Pacchioni, N. Rösch, Chem. Phys. Lett. 275 (1997) 245.
[44] E. Heifets, E.A. Kotomin, R. Orlando, J. Phys.: Condensed Matter 8 (1996) 6577.
[45] E. Heifets, Yu.F. Zhukovskii, E.A. Kotomin, M. Causa, Chem. Phys. Lett. 283 (1998) 395.
[46] J. Purton, S.C. Parker, D.W. Bullett, J. Phys.: Condensed Matter 9 (1997) 5709.
[47] R. Dovesi, V.R. Saunders, C. Roetti, M. Causá, N.M. Harrison, R. Orlando, E. Aprá, CRYSTAL-95 User Manual, University of Turin, 1996.
[48] M. Causá, A. Zupan, Chem. Phys. Lett. 220 (1994) 145.
[49] J.P. Perdew, Y. Wang, Phys. Rev. B 45 (1991) 13 244.
[50] M. Causá, R. Dovesi, C. Pisani, C. Roetti, Surf. Sci. 175 (1986) 551.
[51] P.J. Hay, W.R. Wadt, J. Chem. Phys. 82 (1985) 284.
[52] E. Aprá, E.V. Stefanovich, R. Dovesi, C. Roetti, Chem. Phys. Lett. 186 (1991) 329.
[53] R.W.G. Wyckoff, Crystal Structures, 2nd edition. vol. 1 Wiley-Interscience, New York, 1963.
[54] M. Causá, E.A. Kotomin, C. Pisani, C. Roetti, J. Phys. C. 20 (1977) 4391.
[55] P. Guenard, G. Renaud, B. Villette, Physica B 221 (1996) 205.
[56] C. Kaden, P. Ruggerone, J.P. Toennies, G. Zhang, G. Benedek, Phys. Rev. B 46 (1992) 13 509.
[57] R.W. Grimes, C.R.A. Catlow, A.M. Stoneham, J. Phys.: Condensed Matter 1 (1989) 7367.
[58] J.-W. He, P.J. Møller, Chem. Phys. Lett. 129 (1986) 13.
[59] J.-W. He, P.J. Møller, Surf. Sci. 178 (1986) 934.
[60] J.-W. He, P.J. Møller, Surf. Sci. 180 (1987) 934.
[61] I. Astrup, P.J. Møller, Appl. Surf. Sci. 33–34 (1988) 143.
[62] M. Meunier, C.R. Henry, Surf. Sci. 307 (1994) 514.